

Medical Image Segmentation using Level Sets

Technical Report #CS-2008-12

Tenn Francis Chen

Abstract

Segmentation is a vital aspect of medical imaging. It aids in the visualization of medical data and diagnostics of various diseases. This report presents an implementation of a level set approach for active contour image segmentation. This method is originally developed by Osher and Sethian and then applied to image segmentation by Malladi. No requirements about objects' shape and allowance for very flexible topology change are key advantages for this method.

1 Introduction

Segmentation is defined as partitioning portions of an image. It adds structure to a raw image. In the case of medicine, this can involve identifying which portions of an image is the tumor, or separating white matter from grey matter in a brain scan.

This report presents a simple implementation of an active contour method using level sets and demonstrate this method's abilities. This report will present the formulation of the level set method and issues in numerically implementing the problem. It will then follow with results of the implementation and close with areas for further improvements.

2 The Level Set Method

The segmentation problem reduces to finding curve(s) to enclose regions of interest. Intuitively, we can model the curves directly using control points. However, there are issues involved in updating the control points. For example, if two separate closed curves needed to merge into one, or one needs to split into two, when would this merge/split take place? How would an algorithm detect when to merge or split? After this is detected, data structures for the curve would then be needed to be updated as well. If control points are too close together, how should they be merged? There are solutions to these difficulties [4]. However, these issues can all be alleviated using the level set method.

The level set method was first presented by Osher and Sethian for front propagation, being applied to models of ocean waves and burning flames [4]. Malladi applied it for medical imaging purposes [3]. The idea behind the level set method is to imbed a curve within a surface. In our case, we imbed a two-dimensional curve within a three-dimensional surface. To illustrate this point, Figure 1 shows how a circle can be imbedded in a cone. By indirectly modelling

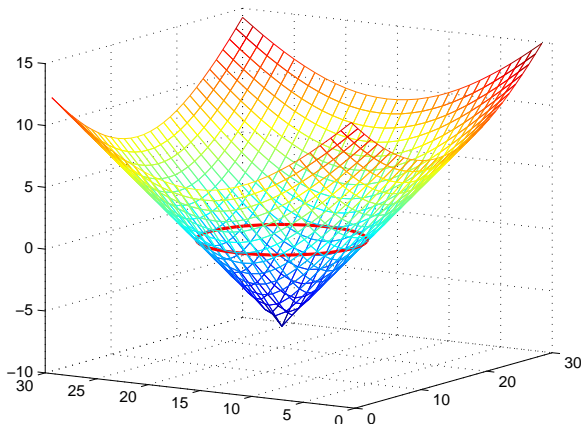


Figure 1: Sketch illustrating a circle embedded within a cone

curves in this way, the above mentioned problems of splitting and merging curves are addressed without the need to treat them as special cases. Figure 2

shows how a curve can split into two by moving along the surface of the level set. Using this idea, we can

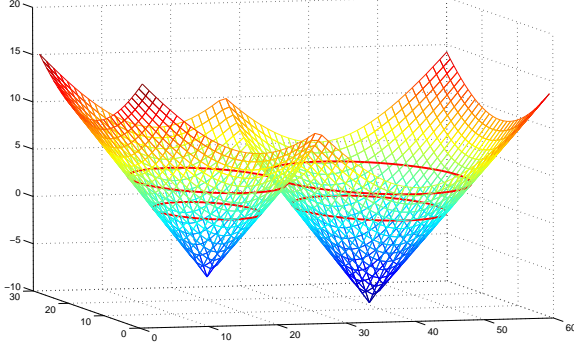


Figure 2: Sketch illustrating how one closed contour embedded in a surface is related to two closed contours on another level

morph the surface to achieve our desired topology at a specific contour level.

2.1 Formulation

In this section, we will describe how the level set method is formulated [3]. We define the segmentation boundary as part of a surface where the contour level is 0, *i.e.*, the zero level set. Let ϕ represent the implicit surface such that

$$\phi(\mathbf{x}, t) = \pm d$$

where \mathbf{x} is a position in our domain (the image), t is time, and d is the distance between position \mathbf{x} and the zero level set. The sign in front of d is positive if \mathbf{x} is outside zero level set. Otherwise, the sign is negative. Note that the curve of interest is then marked by positions where $\phi = 0$.

To evolve ϕ over time, use the chain rule:

$$\begin{aligned} \phi_t + \phi_x x_t + \phi_y y_t &= 0 \\ \phi_t + (x_t, y_t) \cdot \nabla \phi &= 0. \end{aligned}$$

Now, let $(x_t, y_t) = \mathbf{n} + \mathbf{s}$ where \mathbf{n} is the vector normal to the front at point \mathbf{x} and \mathbf{s} is some arbitrary vector. Note that since \mathbf{n} and \mathbf{s} are defined over the entire domain of \mathbf{x} , they are actually vector fields. The above equation can then be written as

$$\begin{aligned} \phi_t + (\mathbf{n} + \mathbf{s}) \cdot \nabla \phi &= 0 \\ \phi_t + \mathbf{n} \cdot \nabla \phi + \mathbf{s} \cdot \nabla \phi &= 0 \\ \phi_t + V_n |\nabla \phi| + \mathbf{s} \cdot \nabla \phi &= 0 \end{aligned} \quad (1)$$

where V_n is some scalar [1]. The two values, V_n and \mathbf{s} , can be viewed as two independent forces that evolve the surface. The scalar V_n will control how fast the surface will move in the normal direction. The vector \mathbf{s} will be another force that dictates both direction and speed of evolution. The partial differential equation can then be solved when provided an initial condition, $\phi(\mathbf{x}, t = 0)$. Thus, the segmentation problem reduces to an initial value problem. This is the formulation used in the implementation presented within this report.

This formulation is to allow for a default expansion or contraction of the level set when no features are present in the image using V_n . When image details are present, V_n can fall off towards 0, and the vector \mathbf{s} take over to lock the level set on to the actual edges.

A valid question is to why not use only one of the forces? By using only V_n , the normal force may be too great for weaker edges. To solve this, the effect of V_n may be cut off early, shown in Figure 3. However,

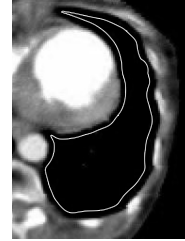


Figure 3: Final result of a segmentation using only normal force. The results are nice, but note the small margin that this segmentation leaves.

this leaves a margin at the edges. When \mathbf{s} is included, the front will converge to the edges.

On the other hand, it is possible to generate a full vector field that covers the entire domain and use only that. Ma and Manjunath [2] describes one such implementation. However, under such a scheme, a front may stop evolving at a position that is equidistant from two edges, a separatrix of the vector field. This problem is seen in Figure 4. At such a position, either edge seems like a viable option to evolve to, and the front will stop moving. An even worse scenario exists if the zero level set is influenced only by vectors of only one edge; the entire set will collapse into that edge. This may occur if the zero level set is close to only one side of some shape in the image. The solution to this problem is to introduce the normal



Figure 4: Final result of a segmentation using only vector field force. Note the upper edge of the segmentation, unable to decide whether to move up or down.

force.

3 Implementation

We can solve Equation 1 using finite difference on a discrete spatial grid in the domain of \mathbf{x} . Let $\phi(\mathbf{x}, n\Delta t) = \phi_{\mathbf{x}}^n$ where Δt is the time step. Then for spatial grid node $\mathbf{x} = ij$, ϕ can be calculated by

$$\begin{aligned} \frac{\phi_{ij}^{n+1} - \phi_{ij}^n}{\Delta t} + (V_n)_{ij} |\nabla \phi_{ij}^n| + \mathbf{s}_{ij} \cdot \nabla \phi_{ij}^n &= 0 \\ \phi_{ij}^{n+1} = \phi_{ij}^n - \Delta t [(V_n)_{ij} |\nabla \phi_{ij}^n| + \mathbf{s}_{ij} \cdot \nabla \phi_{ij}^n] \end{aligned} \quad (2)$$

where $\nabla \phi_{ij}^n$ is calculated using a suitable finite difference scheme. The choice of a scheme is discussed in Section 3.3.

3.1 Normal Speed and Vector Field

For default expansion, we implementation V_n and \mathbf{s} as

$$\begin{aligned} \nabla I^G &= (I_x^G, I_y^G) \\ V_n &= \exp(-\alpha |\nabla I^G|) \\ \mathbf{s} &= \beta \nabla |\nabla I^G| \end{aligned}$$

where I^G is the input image blurred with a Gaussian filter, α is a constant for controlling how fast V_n approaches 0 when an edge is encountered in the image and β is a constant for controlling the strength of \mathbf{s} . This requires 3 parameters: α , β and plus a σ , the standard deviation of the Gaussian filter. We see that when the input image has a small gradient (no

edges), V_n approaches 1 and \mathbf{s} approaches $\mathbf{0}$. However, when nearing an edge, V_n will approach zero, while \mathbf{s} will point towards the edge. A larger α will let V_n approach 0 at a faster rate. On the other hand a smaller σ will preserve more details of the original image, but might produce more ragged edges. Note for default contraction, V_n is multiplied by -1. We calculate these values using central difference:

$$\begin{aligned} (I_x^G)_{ij} &= \frac{I_{i+1,j}^G - I_{i-1,j}^G}{2} \\ (I_y^G)_{ij} &= \frac{I_{i,j+1}^G - I_{i,j-1}^G}{2} \\ |\nabla I^G|_{ij} &= \sqrt{(I_x^G)_{ij}^2 + (I_y^G)_{ij}^2} \\ (V_n)_{ij} &= \exp(-\alpha |\nabla I^G|) \\ (|\nabla I^G|_x)_{ij} &= \frac{|\nabla I^G|_{i+1,j} - |\nabla I^G|_{i-1,j}}{2} \\ (|\nabla I^G|_y)_{ij} &= \frac{|\nabla I^G|_{i,j+1} - |\nabla I^G|_{i,j-1}}{2} \\ \mathbf{s}_{ij} &= \beta ((|\nabla I^G|_x)_{ij}, (|\nabla I^G|_y)_{ij}). \end{aligned}$$

3.2 Entropy Condition

Consider

$$\begin{aligned} u_t(x, t) &= -a(x)u_x(x, t) \\ a(x) &= \begin{cases} -1, & x < 0 \\ 1, & x > 0 \end{cases} \end{aligned} \quad (3)$$

The slope of the characteristic curves are

$$\frac{dt}{dx} = \begin{cases} -1, & x < 0 \\ 1, & x > 0 \end{cases}$$

A sketch of the characteristic curves are shown in Figure 5. Note the empty gap in the figure. In general,

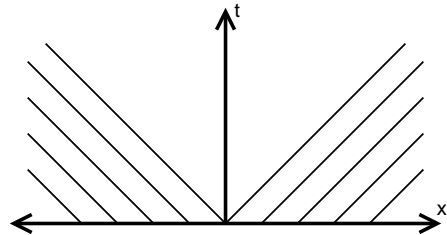


Figure 5: Sketch showing characteristic curves with a gap, implying non-unique solutions

there is no unique solution; different characteristic

curves can fill the gap [4]. However, an additional condition, the entropy condition, can be added. Consider the viscous non-linear wave equation:

$$u_t(x, t) + u(x, t)u_x(x, t) = \epsilon u_{xx}(x, t)$$

Introducing the viscosity term, $\epsilon u_{xx}(x, t)$, converts our equation from a hyperbolic into a parabolic type, which ensures an unique solution. This term will introduce a rarefaction of characteristics in the empty gap, illustrated by Figure 6. We will discuss in Sec-

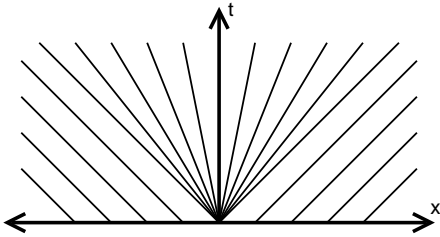


Figure 6: Sketch of characteristic curves with rarefaction wave, implying unique solution

tion 3.3 as to how we will introduce this viscosity term.

3.3 The Upwind Scheme

When implementing Equation 2, special attention should be given to how $\nabla \phi_{ij}^n$ is calculated. For simplicity, we refer to the one-dimensional function u . We have a few options to calculate its derivative:

$$\begin{aligned} D_x^0 u_i &= \frac{u_{i+1} - u_{i-1}}{2\Delta x} \\ D_x^+ u_i &= \frac{u_{i+1} - u_i}{\Delta x} \\ D_x^- u_i &= \frac{u_i - u_{i-1}}{\Delta x}. \end{aligned}$$

These are known as central difference, forward difference, and backward difference respectively. Which one should we choose?

Consider the one-dimensional wave equation:

$$\begin{aligned} u_t(x, t) + u_x(x, t) &= 0 \\ u(x, 0) &= f(x) \end{aligned}$$

where the exact solution is $u(x, t) = f(x - t) = u(x - t, 0)$ and characteristic curves have slope 1. Now, consider a point A on a characteristic curve q . The value at A can be traced back along q to a

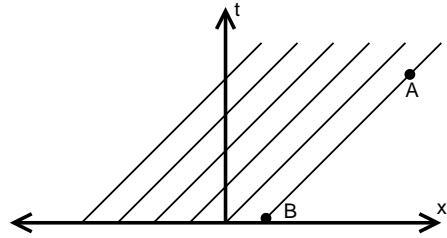


Figure 7: Sketch of characteristic curves. Note B is in the domain of dependence of A .

point, B , where $t = 0$ (See Figure 7). We can say B is in the domain of dependence of A , i.e., A depends on B . Note that information flows from the left to the right.

Taking this into consideration, we should use an approximation scheme that propagates information in the corresponding direction. In the example used, the information flows from the left to the right. Therefore, we use backward difference. In general, information can flow from the right as well; forward difference may be needed.

To illustrate, recall Equation 3. Note that it has characteristic curves of slope 1 and -1. To apply both forward and backward difference, we solve it using the following:

$$\frac{u_i^{n+1} - u_i^n}{\Delta t} = -(\max(a_i, 0)D_x^- u_i^n + \min(a_i, 0)D_x^+ u_i^n)$$

or equivalently

$$u_i^{n+1} = u_i^n - \frac{\Delta t}{\Delta x} \left(\frac{a_i}{2}(u_{i+1}^n - u_{i-1}^n) - \frac{|a_i|}{2}(u_{i+1}^n - 2u_i^n + u_{i-1}^n) \right) \quad (4)$$

where $u_i^n = u(i, n)$ and $a_i = a(i)$. This approach is known as the upwind scheme. Note the last term on the right of Equation 4 is a second order term that corresponds to the viscosity term mentioned in Section 3.2 [1].

Returning to our original problem in two dimensions, we can calculate $\mathbf{s} \cdot \nabla \phi$ for every grid point

as

$$\begin{aligned}
\mathbf{s} \cdot \nabla \phi &= \mathbf{s} \cdot (\phi_x, \phi_y) \\
&= \beta(|\nabla I^G|_x, |\nabla I^G|_y) \cdot (\phi_x, \phi_y) \\
&= \beta[\max(0, |\nabla I^G|_x) D_x^- \phi \\
&\quad + \min(0, |\nabla I^G|_x) D_x^+ \phi \\
&\quad + \max(0, |\nabla I^G|_y) D_y^- \phi \\
&\quad + \min(0, |\nabla I^G|_y) D_y^+ \phi].
\end{aligned}$$

We calculate $V_n |\nabla \phi|$ in a similar fashion:

$$V_n |\nabla \phi| = \sqrt{\phi_1^2 + \phi_2^2}$$

where

$$\begin{aligned}
\phi_1 &= \max(0, V_n) D_x^- \phi + \min(0, V_n) D_x^+ \phi \\
\phi_2 &= \max(0, V_n) D_y^- \phi + \min(0, V_n) D_y^+ \phi.
\end{aligned}$$

3.4 The CFL Condition

Note that we are using a discrete method to solve a continuous problem. Courant, Friedrichs, and Lewy noted that there is a necessary condition to preserve stability when solving problems in this way. The condition has since then been referred to as the Courant-Friedrichs-Lewy (CFL) condition. They noted that the numerical domain of dependence needs to include the analytical domain of dependence. This idea is shown in Figure 8. In our case, a level set may only

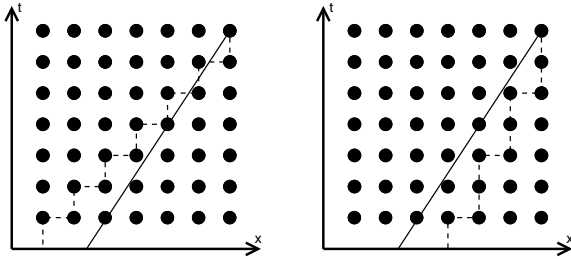


Figure 8: In both sketches, let the solid line represent the analytical domain of dependence and the dashed line be numerical domain of dependence. Note in the left sketch, $\Delta t = 1$ $\Delta t = 2$ on the right. On the left the numerical domain of dependence includes the analytical domain of dependence, satisfying the CFL condition. The CFL condition is violated on the right.

evolve to an adjacent grid point [5, 6]. This is necessary since each point is updated by only its neighbouring points; information should not be moving

faster than one grid point per time step. To prevent the appearance of instabilities, the timestep is implemented as

$$\Delta t = \frac{c}{\max\{|V_n|\} + \max\{|\mathbf{s}|\}}$$

where $0 < c \leq 1$ is some scaling constant set by the user.

4 Results

Here we provide some results of our implementation. It was noted that the curve can split to two different curves. This is shown in Figure 9. This example also contracts the contour by default by setting the V_n to be negative. An example of the contours merging is shown in Figure 10. In Figure 11, we also see how a contour can wrap around a region of non-interest. Some error in the segmentation is also seen; a little bit of the rig cage is included on the right of the contour. For a more complex examples, the white matter being segmented within a human brain is shown in Figures 12 and 13.

5 Possible Improvements

Currently, at each iteration of the algorithm, every point within the domain is updated. However, the final result is only interested in the zero level set. Therefore, the current implementation is very inefficient. A way to improve efficiency is to evolve the surface only on a narrow band around the current zero level set for the current iteration. This relieves the needless computation on irrelevant parts of the domain. This is known as the narrow band scheme [3, 6].

Another way to improve the current implementation is to expand to higher dimensions. Note that the formulation of the level set method (Equation 1) has no limit on the dimensions. Indeed, level sets has been applied to three-dimensional data sets [5]. For example level set approach is able to segment a tumor within a three-dimensional model of a brain.

Additional forces and constraints can also be added to refine the model. For example, a curvature force can be included to prevent sharp corners from forming [3]. Also, although no prior knowledge of the image is required, it can be useful. Referring to Figure 11, if knowledge of the ribs are used, we can set

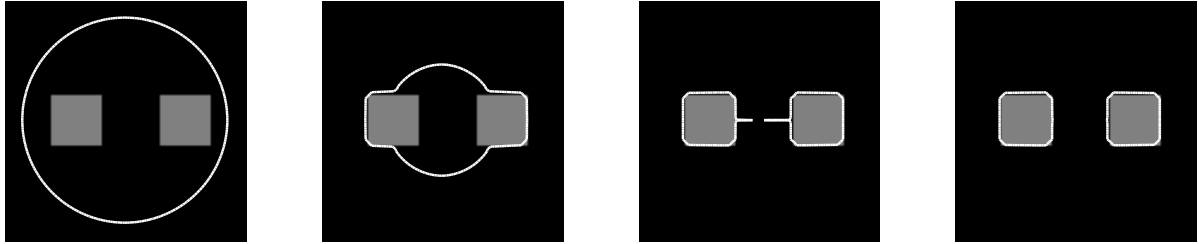


Figure 9: Demonstration of a zero level set contracting and splitting. Temporal ordering is from left to right. This image is an artificial image of two blocks.

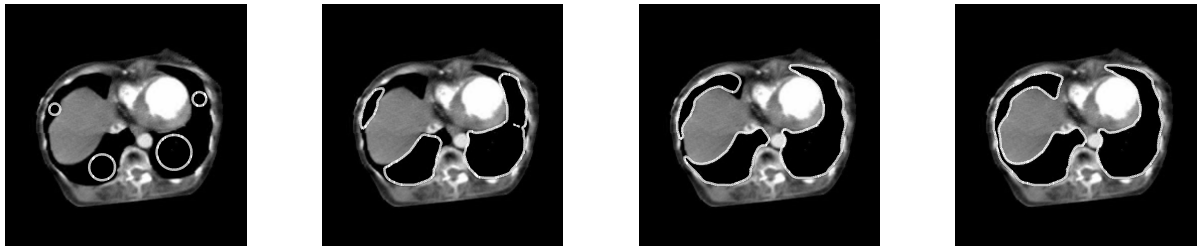


Figure 10: Demonstration of zero level sets expanding and merging. Temporal ordering is from left to right. This image is a medical scan of the chest, where the feet are pointed out of the viewing plane. The lungs are being segmented.

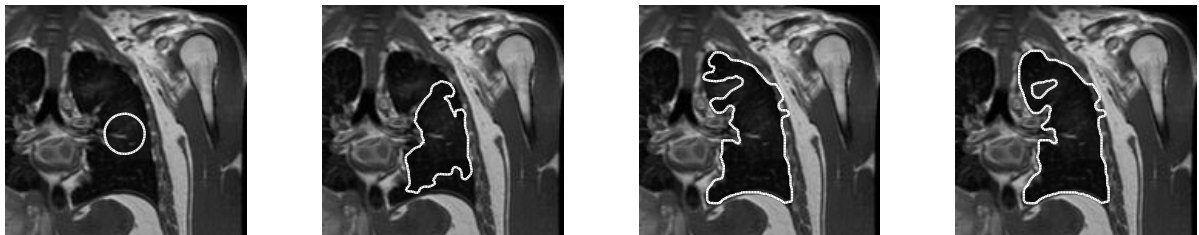


Figure 11: Demonstration of a zero wrapping around a region of non-interest. Temporal ordering is from left to right. This image is a medical scan of the chest, top-down view. A lung is being segmented. Note that the segmentation also included a little bit of a ribs on the right.

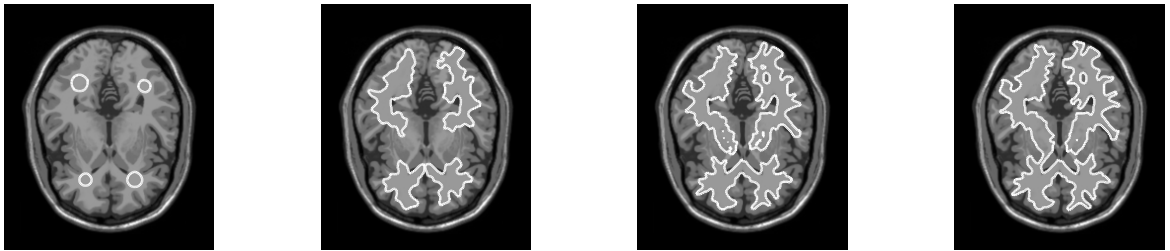


Figure 12: Demonstration of segmentation of white matter in a brain. Temporal ordering is from left to right.

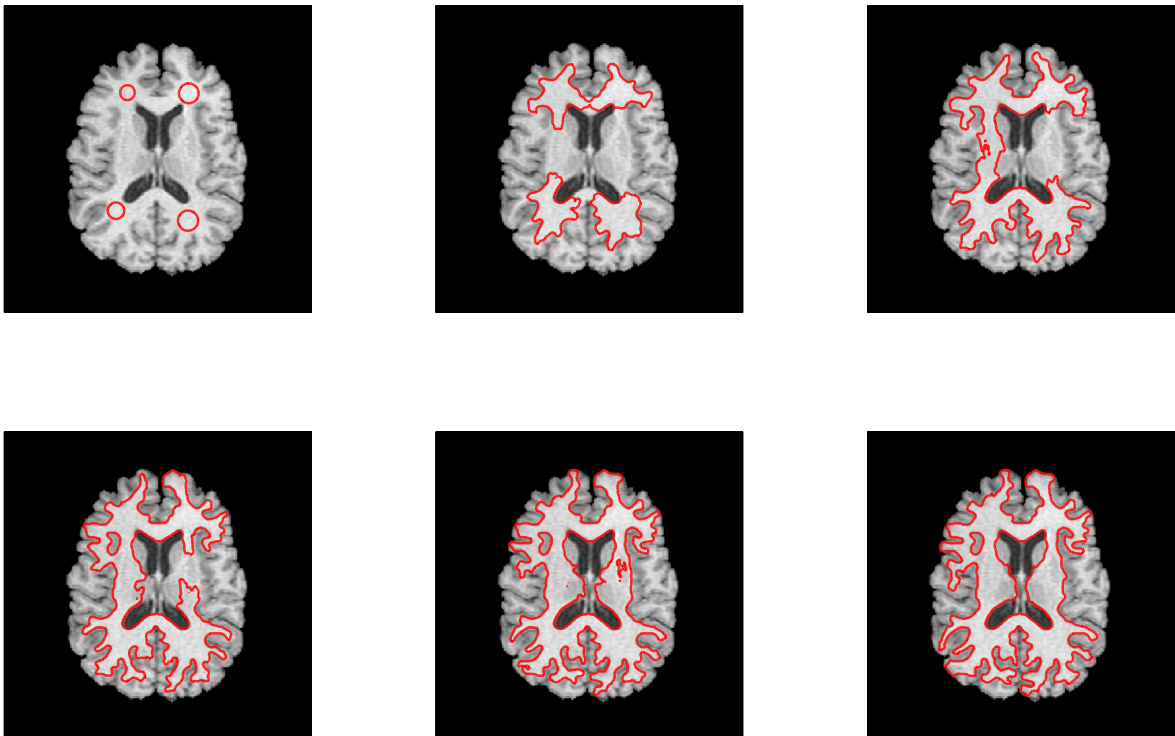


Figure 13: Demonstration of segmentation of white matter in a brain. Temporal ordering is from left to right, top to bottom.

a repelling force along the wall of the ribs to prevent over-segmentation.

6 Conclusion

A simple and intuitive level set method has been implemented. The results shown demonstrated the versatility of the method by the complex shapes it has extracted. The implementation has demonstrated the method's flexible topology adaptability and no requirement of any knowledge of the target shape. Despite its simplicity, it has generated some rather nice results. However, there is room for improvement but the capabilities and possibilities of this approach have been clearly demonstrated.

References

- [1] KIMMEL, R. *Numerical geometry of images: theory, algorithms, and applications*. Springer, 2003.
- [2] MA, W. Y., AND MANJUNATH, B. S. Edge flow: A framework of boundary detection and image segmentation. *IEEE Proc. on Computer Vision and Pattern Recognition* (1997), 744–749.
- [3] MALLADI, R., SETHIAN, J. A., AND VEMURI, B. Shape modeling with front propagation: A level set approach. *IEEE Transactions on Pattern Analysis and Machine Intelligence* 17, 2 (1995), 158 – 175.
- [4] SETHIAN, J. A. *Level set methods and fast marching methods: evolving interfaces in computational geometry, fluid mechanics, computer vision, and materials science*. Cambridge Universtiy Press, 1999.
- [5] WEST, J. J. Application of the level set method to hydrocephalus: Simulating the motion of the ventricles. Master's thesis, University of Waterloo, 2004.
- [6] YOO, T. S. *Insight into images: principles and practice for segmentation, registration, and image analysis*. A K Peters, Ltd., 2004.